



Improved simplified response methods to blast loading

Prepared by the **Steel Construction Institute**
for the Health and Safety Executive 2006

RESEARCH REPORT 435



Improved simplified response methods to blast loading

The Steel Construction Institute
Silwood Park
Ascot
Berkshire
SL5 7QN

This report describes the second-stage extension of a sophisticated SDOF model for steel members subject to explosion loading [1], previously developed under commission from the Steel Construction Institute.

The previous model [1] accounted for i) generalised support conditions for bending and axial actions, and ii) the catenary effect in axially-restrained members, under uniformly distributed (UDL), blast loading. However, this model did not incorporate material rate sensitivity, which has considerable influence on the blast response of steel members. This work extends the previous model [1] to deal with the strain-rate effect, and to provide more rational ductility measures than possible with rate-insensitive modelling.

The report proceeds by providing an overview of the problem characteristics as well as the formulation method used in developing the new SDOF model, where consideration is given to material rate sensitivity in accordance with the Cowper-Symonds model [2]. The details of the overall model are then provided, mainly in the form of parametric tables, covering both the bending and catenary stages of the plastic rate-sensitive member response. Finally, several verification and application examples are provided, with particular emphasis given to the new developments, where comparisons are made against the nonlinear finite element analysis program ADAPTIC [3]. These examples demonstrate the calculation process involved in applying the new SDOF model, and illustrate the very good accuracy which the new model achieves.

This report and the work it describes were funded by the Health and Safety Executive (HSE). Its contents, including any opinions and/or conclusions expressed, are those of the author alone and do not necessarily reflect HSE policy.

© Crown copyright 2006

First published 2006

All rights reserved. No part of this publication may be reproduced, stored in a retrieval system, or transmitted in any form or by any means (electronic, mechanical, photocopying, recording or otherwise) without the prior written permission of the copyright owner.

Applications for reproduction should be made in writing to:
Licensing Division, Her Majesty's Stationery Office,
St Clements House, 2-16 Colegate, Norwich NR3 1BQ
or by e-mail to hmsolicensing@cabinet-office.x.gsi.gov.uk

CONTENTS

EXECUTIVE SUMMARY	V
1 INTRODUCTION	1
2 PROBLEM CHARACTERISTICS AND ASSUMPTIONS	3
3 FORMULATION METHOD	6
3.1 CROSS-SECTIONAL RESPONSE	6
3.2 BENDING STAGE	7
3.3 CATENARY STAGE	9
4 CROSS-SECTIONAL RESPONSE	12
4.1 MAJOR-AXIS BENDING	12
4.2 MINOR-AXIS BENDING	13
5 DYNAMIC STRENGTH	15
5.1 BENDING STAGE	15
5.2 CATENARY STAGE	15
5.3 EVALUATION OF MODEL PARAMETERS	16
6 DUCTILITY MEASURES	19
7 EXAMPLES AND VERIFICATION	22
7.1 CROSS-SECTION RESPONSE	22
7.2 UDL BLAST	22
8 CONCLUSION	28
Appendix 1 REFERENCES	30
Appendix 2 NOTATION	32
Appendix 3 FIGURES	38
Appendix 4 TABLES	44

EXECUTIVE SUMMARY

The most widely applied SDOF model has so far been that of Biggs, which suffers from the following shortcomings:

- 1) It does not account for different moment capacities and rotational stiffnesses at the two supports
- 2) It ignores the catenary effect, which has a significant influence on the large displacement member response in the presence of axial restraint at the supports.
- 3) It ignores the influence of material rate-sensitivity
- 4) It ignores the influence of strain-hardening, through assuming elastic perfectly-plastic material and cross-sectional responses.
- 5) It does not account for the beam-column effect in load-bearing members that sustain significant compressive axial forces.

Theoretical developments to address the first two shortcomings were carried out previously and are outlined in an earlier document [1]. The present work addresses the third shortcoming and provides the theoretical background as well as a step-by-step procedure for solving SDOF models with strain-rate effects. The model was validated by comparison against results from the software ADAPTIC. The results between the SDOF model and ADAPTIC exhibited good agreement.

1 INTRODUCTION

This report describes the second-stage extension of a sophisticated SDOF model for steel members subject to explosion loading [1], previously developed under commission from the Steel Construction Institute.

The previous model [1] accounted for i) generalised support conditions for bending and axial actions, and ii) the catenary effect in axially-restrained members, under uniformly distributed (UDL), blast loading. However, this model did not incorporate material rate sensitivity, which has considerable influence on the blast response of steel members. This work extends the previous model [1] to deal with the strain-rate effect, and to provide more rational ductility measures than possible with rate-insensitive modelling.

The report proceeds by providing an overview of the problem characteristics as well as the formulation method used in developing the new SDOF model, where consideration is given to material rate sensitivity in accordance with the Cowper-Symonds model [2]. The details of the overall model are then provided, mainly in the form of parametric tables, covering both the bending and catenary stages of the plastic rate-sensitive member response. Finally, several verification and application examples are provided, with particular emphasis given to the new developments, where comparisons are made against the nonlinear finite element analysis program ADAPTIC [3]. These examples demonstrate the calculation process involved in applying the new SDOF model, and illustrate the very good accuracy which the new model achieves.

2 PROBLEM CHARACTERISTICS AND ASSUMPTIONS

A simplified SDOF model was previously formulated [1] for a steel beam under dynamic loading, where the problem characteristics were as follows:

- The member has uniform cross-sectional properties along its length.
- The cross-sectional response is elastic/perfectly plastic (i.e. no strain hardening).
- The member has two end supports where transverse displacements are restrained (Figure 1).
- Arbitrary elastic perfectly plastic conditions are considered for the two end supports for both rotational and axial deformations (Figure 1).
- The strain-rate effect is ignored.
- The dynamic blast loading is UDL.
- The initial static loading is UDL.
- The mass is uniformly distributed along the member length.
- Both bending and catenary actions are considered.

The following assumptions were further made [1] to facilitate the formulation of a relatively uncomplicated model which should nevertheless capture the essential problem characteristics:

- The member response under initial static loading is elastic.
- The location of the internal plastic hinge is governed by the blast load configuration.
- The interaction between the plastic bending moment and axial force is linear (Figure 2).

The previous model is extended here to account for the strain-rate effect, where the following additional assumptions are made:

- Material rate sensitivity is governed by the Cowper-Symonds model [2].
- The cross-sectional response under a constant deformation rate is elastic/perfectly plastic, with an enhanced dynamic plastic strength that is determined from rigid/plastic theory as a function of the deformation rate.
- The plastic curvature rate decreases rapidly along the member away from the point of maximum bending moment, justifying the related assumption of lumped plastic-hinge rotation.
- The dynamic strength of a plastic hinge remains constant over the response duration, and is determined from a deformation rate associated with a plastic collapse mechanism and an average displacement rate, accounting, where appropriate, for the plastic-hinge length.
- Where the static plastic capacity of a support is less than that of the beam, the plastic hinge is completely in the support (i.e. outside the beam), and the corresponding dynamic strength is obtained directly in terms of the support deformation rate.
- The shape of the plastic bending moment diagram is governed by the blast load configuration.

Full details of the notation employed throughout this work are provided in Appendix 2.

It is noted that the formulation can be applied to all structural steel members that can be reduced to a single-degree-of-freedom system including corrugated blast walls. The formulation allows for different boundary conditions to be accounted including finite axial and rotational stiffnesses.

In addition, stainless steel members can also be analysed by inserting the appropriate values for the material properties namely the Young's Modulus, 0.2% proof strength, ultimate strain and Cowper-Symonds constants.

3 FORMULATION METHOD

This work extends a previous SDOF model [1] to deal with the influence of material rate sensitivity on the blast response of steel members. With the strain-rate effect defined on the material level, according to the Cowper-Symonds model [2], its influence is first considered on the cross-sectional response and subsequently on the overall member response.

3.1 CROSS-SECTIONAL RESPONSE

The material response under a constant strain rate ($\dot{\epsilon}$) can be idealised, in the absence of strain hardening, as elastic/perfectly plastic with an enhanced dynamic yield strength (σ_d) (Figure 3). According to the Cowper-Symonds model [2]:

$$(1): \quad \sigma_d = \sigma_y \left(1 + \left(\frac{\dot{\epsilon}}{D} \right)^{1/n} \right)$$

where n and D are material rate-sensitivity parameters, and σ_y is the static yield strength. For mild steel ($n = 5$) and ($D = 40 \text{ sec}^{-1}$), though the extended SDOF model is formulated for generic n and D parameters, and is therefore also applicable to other materials provided ($n \geq 4$).

The cross-sectional response under a constant deformation rate can also be idealised as elastic/perfectly plastic. The enhanced dynamic plastic strength can be obtained from first relating the material strain rates to the generalised cross-section plastic strain rates (Figure 4):

$$(2): \quad \dot{\epsilon} = \dot{\epsilon}_p = \dot{\epsilon}_{cp} - y \dot{\kappa}_p$$

where $\dot{\epsilon}_{cp}$ is the centroidal axial plastic strain rate, $\dot{\kappa}_p$ is the plastic curvature rate, and y is the distance of a material fibre from the reference centroidal line. The material plastic strain rate ($\dot{\epsilon}_p$) is identical to $\dot{\epsilon}$ in the plastic range, since material strain hardening is ignored.

The dynamic plastic moment and axial force capacities can then be determined from consideration of the plastic stress distributions under constant $\dot{\kappa}_p$ and $\dot{\epsilon}_{cp}$, respectively:

$$(3): \quad M_d = \int -\sigma_d y dA = \int \pm \sigma_y \left(1 + \left(\frac{\pm y \dot{\kappa}_p}{D} \right)^{1/n} \right) y dA = M_p \left(1 + \left(\frac{\dot{\kappa}_p}{D_\kappa} \right)^{1/n} \right)$$

$$(4): \quad F_d = \int \sigma_d dA = \int \sigma_y \left(1 + \left(\frac{\dot{\epsilon}_{cp}}{D} \right)^{1/n} \right) dA = F_p \left(1 + \left(\frac{\dot{\epsilon}_{cp}}{D} \right)^{1/n} \right)$$

where $\dot{\kappa}_p$ and $\dot{\epsilon}_{cp}$ are considered in absolute value, M_p and F_p are the static plastic bending moment and axial force capacities, respectively, and D_κ is a rate-sensitivity parameter for plastic bending which depends on the cross-section shape as determined in Section 4.

It is noted that (3) assumes that the position of the neutral axis is not influenced by material rate sensitivity, which is valid for bending about an axis of symmetry. Although for asymmetric cross-sections the position of the neutral axis can vary with the plastic curvature rate, the influence of such variation on dynamic magnification of the plastic moment capacity can be realistically neglected, and hence (3) is also applicable to moderately asymmetric cross-sections.

Finally, the interaction between the dynamic plastic moment and axial force is realistically assumed to have the same shape as the static interaction curve (Figure 5), where the transition between full plastic bending and plastic axial resistance is governed by:

$$(5): \quad \begin{cases} \dot{\epsilon}_{cp} < r_p \dot{\kappa}_p \Rightarrow M = M_d \\ \dot{\epsilon}_{cp} = r_p \dot{\kappa}_p \Rightarrow M + r_p F = M_d \end{cases}$$

with,

$$(6): \quad r_p = \frac{M_p}{F_p}$$

In view of the above, the principles used for formulating the previous rate-insensitive SDOF model [1] remain valid, provided the static cross-section capacities, M_p and F_p , are replaced by their dynamic equivalents, M_d and F_d , taking into account the deformation rate.

3.2 BENDING STAGE

The dynamic moment capacities at the member plastic hinges are obtained as the steady-state solution associated with a collapse mechanism subject to an average displacement rate. A number of cases arise depending on whether the plastic hinge at a member end is in the beam or in the support, as determined by the relative static plastic bending capacities of the support to that of the beam. The case of a plastic hinge in the beam at the left end but in the support at the right end is illustrated in Figure 6. For a given dynamic plastic bending moment diagram, the plastic-hinge lengths in the beam can be determined where appropriate, and the rotation rate of these plastic hinges can be obtained.

Considering first the internal plastic hinge (Figure 6), the rotation rate is determined as the integral of the plastic curvature rate over the plastic-hinge length:

$$(7): \quad \dot{\theta}_p = \int_{h_p} \dot{\kappa}_p dx = \int_{h_p} D_\kappa \left(\frac{M}{M_p} - 1 \right)^n dx = \mathcal{O}_p \left(\frac{M_d}{M_p}, h_p \right)$$

For the plastic hinge at the left end, the determination of the rotation rate depends on whether the plastic hinge is inside the beam (Figure 6):

$$(8.a): \quad M_p^1 = M_p \Rightarrow \dot{\theta}_p^1 = \int_{h_p^1} \dot{\kappa}_p^1 dx = \int_{h_p^1} D_\kappa \left(\frac{M}{M_p} - 1 \right)^n dx = \mathcal{O}_p^1 \left(\frac{M_d^1}{M_p^1}, h_p^1 \right)$$

or in the support, in which case the rotation rate is directly related to the dynamic plastic moment as determined by the support characteristics:

$$(8.b): \quad M_p^l < M_p \Rightarrow \dot{\theta}_p^l = \Theta_p^l \left(\frac{M_d^l}{M_p^l} \right)$$

Similarly, for the plastic hinge at the right end, the determination of the rotation rate depends on whether the plastic hinge is inside the beam:

$$(9.a): \quad M_p^r = M_p \Rightarrow \dot{\theta}_p^r = \int_{h_p^r} \dot{\kappa}_p^r dx = \int_{h_p^r} D_\kappa \left(\frac{M}{M_p} - 1 \right)^n dx = \Theta_p^r \left(\frac{M_d^r}{M_p^r}, h_p^r \right)$$

or in the support (Figure 6):

$$(9.b): \quad M_p^r < M_p \Rightarrow \dot{\theta}_p^r = \Theta_p^r \left(\frac{M_d^r}{M_p^r} \right)$$

In the above expressions, h_p^l , h_p and h_p^r are the plastic-hinge lengths corresponding to the zones of the member over which the static plastic bending moment capacity (M_p) is exceeded (Figure 6), and therefore these depend on the dynamic bending moment diagram as defined by M_d^l , M_d and M_d^r . Furthermore, Θ_p^l , Θ_p and Θ_p^r are highly nonlinear functions which depend on the variation of the bending moment over the corresponding plastic-hinge length. With each of $\dot{\theta}_p^l$, $\dot{\theta}_p$ and $\dot{\theta}_p^r$ related to the member displacement rate (\dot{v}^m), the nonlinear equations (7) to (9) can be solved for M_d^l , M_d and M_d^r in terms of \dot{v}^m , though an exact solution can be very demanding, if not impossible. However, good solution accuracy can be achieved through appropriate simplifications, particularly with regard to relating the plastic-hinge lengths to the dynamic bending moments. Consequently, equations (7) to (9) can be expressed in the following general form:

$$(10): \quad \dot{\theta}_p^l = D_\theta^l \left(\frac{M_d^l}{M_p^l} - 1 \right)^{n_m^l}$$

$$(11): \quad \dot{\theta}_p = D_\theta \left(\frac{M_d}{M_p} - 1 \right)^{n_m}$$

$$(12): \quad \dot{\theta}_p^r = D_\theta^r \left(\frac{M_d^r}{M_p^r} - 1 \right)^{n_m^r}$$

where (D_{θ}^l, n_m^l) , (D_{θ}, n_m) and (D_{θ}^r, n_m^r) are parameters that are either given (for an end plastic hinge in the support) or derived (for a plastic hinge in the beam).

With $\dot{\theta}_p^l$, $\dot{\theta}_p$ and $\dot{\theta}_p^r$ depending on \dot{v}^m according to the plastic collapse mechanism, the dynamic plastic moment capacities can be determined from (10) to (12), as presented in Section 5.

Finally, it should be noted that for the case where an end plastic hinge is in the support ($M_p^l < M_p$ or $M_p^r < M_p$), it is possible for the corresponding dynamic plastic bending moment (M_d^l or M_d^r) to exceed the static plastic bending moment of the beam. Although in such a case, plastic deformation is also induced in the beam at the corresponding end, this would normally be small in comparison with the plastic deformation induced in the support, and is therefore neglected in the extended rate-sensitive SDOF model so as to maintain simplicity without significant compromise to accuracy.

3.3 CATENARY STAGE

With the assumed interaction between the dynamic plastic bending moment and axial force, as discussed in Section 3.1, the first catenary stage is initiated as for the rate-insensitive model when:

$$(13): \quad v^m = r_p^t - v_0^m = (c^l r_p^l + r_p + c^r r_p^r) - v_0^m$$

with,

$$(14): \quad r_p^l = \frac{M_p^l}{F_p^l}; \quad r_p = \frac{M_p}{F_p}; \quad r_p^r = \frac{M_p^r}{F_p^r}$$

where c^l and c^r are weighting parameters that depend on the location of the internal plastic hinge [1], and v_0^m is the reference displacement due to initial static loading. It is noted that, according to (14), the plastic radii are only functions of the static bending and axial capacities of the beam and supports.

For a given dynamic magnification in the static bending strength, as determined in accordance with Section 3.2, the development of an axial force during the first catenary stage leads to a reduction in the bending moments but to an increase in the plastic-hinge lengths. This latter increase would be associated with an increased deformation rate, and hence for a constant deformation rate, as assumed by the extended SDOF model, the dynamic magnification of the static strength should be reduced in the first catenary stage. However, this effect is considered to be negligible, and the complexities associated with its modelling are therefore not justified, particularly in view of the transient nature of the first catenary stage.

The transition between the first and second catenary stages is defined by a dynamic axial force capacity (F_d^m), dependent on the overall plastic axial deformation rate ($\dot{\Delta}_p^t$) and whether the axial plastic deformation is concentrated in any of the supports or spread over the length of the beam. Four cases can be identified as follows:

$$(15.a): \quad F_p^l < F_p^r \leq F_p \Rightarrow \dot{\Delta}_p^t - r_p \dot{\theta}_p - r_p^r \dot{\theta}_p^r = D_\Delta^l \left(\frac{F_d^m}{F_p^l} - 1 \right)^{n_f^l}$$

$$(15.b): \quad F_p^l = F_p^r < F_p \Rightarrow \dot{\Delta}_p^t - r_p \dot{\theta}_p = 2D_\Delta^l \left(\frac{F_d^m}{F_p^l} - 1 \right)^{n_f^l}$$

$$(15.c): \quad F_p^r < F_p^l \leq F_p \Rightarrow \dot{\Delta}_p^t - r_p^l \dot{\theta}_p^l - r_p \dot{\theta}_p = D_\Delta^r \left(\frac{F_d^m}{F_p^r} - 1 \right)^{n_f^r}$$

$$(15.d): \quad F_p^l = F_p^r = F_p \Rightarrow \dot{\Delta}_p^t = LD \left(\frac{F_d^m}{F_p} - 1 \right)^n$$

where (D_Δ^l, n_f^l) and (D_Δ^r, n_f^r) represent axial rate-sensitivity parameters for the left and right supports, respectively.

With $\dot{\Delta}_p^t$, $\dot{\theta}_p^l$, $\dot{\theta}_p$ and $\dot{\theta}_p^r$ related to the reference displacement rate (\dot{v}^m), depending on the plastic collapse mechanism, the dynamic plastic axial capacity can be obtained from one of the applicable equations in (15), as presented for the individual blast loading configurations in Sections 5 to 7.

It is noted that the second case represented by (15.b) corresponds to identical plastic axial response characteristics for the left and right supports, and hence axial plasticity is equally shared between the two supports. Furthermore, as for bending plasticity, the above expressions assume that the localisation of axial plasticity is related to the static rather than the dynamic relative axial capacities of the supports and the beam. This is considered to be a realistic assumption, which avoids major complications without significant compromise to accuracy in the determination of F_d^m .

4 CROSS-SECTIONAL RESPONSE

According to (3), the determination of the dynamic plastic bending moment capacity requires a rate-sensitivity parameter (D_κ), which depends on the cross-sectional shape and the axis of bending. In general, this can be related to the material rate-sensitivity parameter (D) by:

$$(16): \quad D_\kappa = \frac{D}{d_e}$$

where d_e represents an effective distance from the neutral axis.

Two cross-sectional configurations are considered for the enhanced SDOF model, as depicted in Figure 7, with bending about both the major and minor axes considered for the I-section.

4.1 MAJOR-AXIS BENDING

With reference to Figure 7a, for an asymmetric I-section subject to major-axis bending, d_e can be expressed as:

$$(17): \quad d_e = \frac{d_w}{2} \left[\frac{\left(\frac{n w - (n+1)\delta}{2n+1} + 1 \right) \left(1 + \frac{\delta}{w} \right)^{\left(\frac{n+1}{n} \right)} + \left(\frac{n w + (n+1)\delta}{2n+1} + 1 \right) \left(1 - \frac{\delta}{w} \right)^{\left(\frac{n+1}{n} \right)}}{w \left(1 + \frac{\delta}{w} \right) \left(1 - \frac{\delta}{w} \right) + 2} \right]^n$$

where,

$$(18): \quad w = \frac{A_w}{A_f^b + A_f^t}; \quad \delta = \frac{|A_f^b - A_f^t|}{A_f^b + A_f^t}$$

with ($\delta \leq w$) indicating a moderately asymmetric I-section with the neutral axis in the web.

The same expressions (17) and (18) can also be used for the out-of-plane one-way bending of a corrugated wall section (Figure 7b).

For a symmetric I-section subject to major-axis bending, the above expression for d_e simplifies to:

$$(19): \quad d_e = \frac{d_w}{2} \left[1 - \frac{w}{(2n+1)(w+2)} \right]^n$$

such a cross-section being characterised with ($\delta = 0$).

4.2 MINOR-AXIS BENDING

With reference to Figure 7a, for an asymmetric I-section subject to minor-axis bending, d_e can be expressed as:

$$(20): \quad d_e = \frac{1}{2} \left[\frac{2n}{2n+1} \left(\beta (b_f^b)^{1/n} + (1-\beta) (b_f^t)^{1/n} \right) \right]^n$$

where,

$$(21): \quad \beta = \frac{A_f^b b_f^b}{A_f^b b_f^b + A_f^t b_f^t}$$

For a symmetric I-section subject to minor-axis bending, the above expression for d_e simplifies to:

$$(22): \quad d_e = \frac{b_f}{2} \left[\frac{2n}{2n+1} \right]^n$$

with b_f representing the flange width ($b_f = b_f^b = b_f^t$).

5 DYNAMIC STRENGTH

This section describes the evaluation of the dynamic strength characteristics associated with UDL blast, for both the bending and catenary stages. This covers the determination of the dynamic plastic bending moments at the plastic hinges, which are generally related to the plastic-hinge rotation rates according to Table 1, as well as the overall dynamic axial strength, which is generally related to an equivalent plastic axial deformation rate according to Table 2. The evaluation of these entities for UDL blast and their use in rate-sensitive dynamic analysis are discussed hereafter.

5.1 BENDING STAGE

The bending rate-sensitivity parameters ($D_\theta^l, D_\theta, D_\theta^r$) and (n_m^l, n_m, n_m^r), that are required in Table 1 for the evaluation of the dynamic plastic bending moments (M_d^l, M_d, M_d^r) at the three respective plastic hinges, are provided in Table 3.

It is important to note that the dynamic bending strength at a support, M_d^l or M_d^r , is determined from the provided tables only if the corresponding plastic hinge is in the member, as expressed by the condition on the static plastic bending moments ($M_p^l = M_p$) or ($M_p^r = M_p$); otherwise, the plastic hinge is in the support, and the dynamic bending strength is assumed to be given directly in terms of the corresponding plastic rotation rate. For the dynamic bending strength at the internal plastic hinge, a rate parameter (α) reflecting the material rate sensitivity and the quadratic bending moment distribution is also required, which is given by:

$$(23): \quad \alpha = \frac{2 \times 4 \times \dots \times 2n}{3 \times 5 \times \dots \times (2n+1)} = \prod_{j=1}^n \frac{2j}{2j+1} = \frac{(2^n n!)^2}{(2n+1)!}$$

The parameters for the plastic hinges depend on the static bending moment distribution in the plastic collapse mechanism, as expressed by the non-dimensional entities (m_p^l, m_p^r), the material rate parameter (n), and the cross-sectional rate parameter (D_κ) provided in Section 4.

Finally, the plastic-hinge rotation rates ($\dot{\theta}_p^l, \dot{\theta}_p, \dot{\theta}_p^r$) that determine the specific values of the dynamic bending strength (M_d^l, M_d, M_d^r), according to Table 1, are obtained from the reference displacement rate (\dot{v}^m) according to the plastic collapse mechanism, as given in Table 4.

5.2 CATENARY STAGE

The overall dynamic axial strength (F_d^m) is obtained from Table 2, depending on whether full axial plasticity is concentrated in the supports or spread over the member, as governed by the relative values of the static axial strengths (F_p^l, F_p, F_p^r). For this purpose, axial rate parameters (D_Δ^m) and (n_f^m) are first determined, either in terms of corresponding known entities when axial plasticity is localised in the supports, or in terms of the member material rate-sensitivity parameters (D) and (n) when axial plasticity is distributed over the member. Finally, a local

axial deformation rate ($\dot{\Delta}_p^m$) is obtained in terms of the overall axial deformation rate ($\dot{\Delta}_p^t$) and the plastic-hinge rotation rates ($\dot{\theta}_p^l, \dot{\theta}_p, \dot{\theta}_p^r$), which are in turn determined from the reference displacement rate (\dot{v}^m) according to Table 4.

5.3 EVALUATION OF MODEL PARAMETERS

The following steps should be considered for evaluating the dynamic strength characteristics of the SDOF model:

1. *Geometric and structural properties.* Establish $A_f^b, b_f^b, A_f^t, b_f^t, A_w, d_w, L, M_p, F_p, M_p^l, F_p^l, M_p^r, F_p^r, D, n$.
 - For bending and/or axial plastic hinges in the support, ($M_p^l < M_p, M_p^r < M_p, F_p^l < F_p$ and/or $F_p^r < F_p$), establish the respective rate-sensitivity parameters ($[D_{\theta}^l, n_m^l], [D_{\theta}^r, n_m^r], [D_{\Delta}^l, n_f^l]$ and/or $[D_{\Delta}^r, n_f^r]$) from the support characteristics.
2. *Cross-sectional bending rate sensitivity.* Determine D_{κ} from (17), (19) or (20), depending on the cross-section shape and axis of bending, and establish D_{κ} from (16).
3. *Member rate sensitivity.* Establish the member rate-sensitivity parameters for the bending and catenary response.
 - For the bending response, determine $[D_{\theta}^l, n_m^l], [D_{\theta}, n_m]$ and $[D_{\theta}^r, n_m^r]$ from Table 3. The support parameters ($[D_{\theta}^l, n_m^l]$ and/or $[D_{\theta}^r, n_m^r]$) are established here only if the corresponding plastic hinge is in the member according to ($M_p^l = M_p$ and/or $M_p^r = M_p$); otherwise, they are given in step 1.
 - For the catenary response, determine $[D_{\Delta}^m, n_f^m]$ from Table 2, depending on whether axial plasticity is localised in one or both support, or is spread over the member, as governed by the respective conditions ($F_p^l < F_p^r \leq F_p, F_p^l = F_p^r < F_p, F_p^r < F_p^l \leq F_p, F_p^l = F_p^r = F_p$).
4. *Dynamic strengths.* Establish the dynamic bending and catenary strengths for a given reference displacement rate (\dot{v}^m).
 - For the dynamic bending strengths, obtain the plastic-hinge rotation rates ($\dot{\theta}_p^l, \dot{\theta}_p, \dot{\theta}_p^r$) from Table 4, and establish the dynamic bending moment strengths (M_d^l, M_d, M_d^r) from Table 1.

- For the dynamic axial strength, obtain the overall axial deformation rate ($\dot{\Delta}_p^t$) from Table 4, and determine the corresponding local deformation rate ($\dot{\Delta}_p^m$) and the resulting dynamic axial strength (F_d^m) from Table 2.
5. *SDOF model resistance.* Replace the static strengths (M_p^l, M_p, M_p^r, F_p^m) in the previously developed SDOF model [2] with the above dynamic strengths (M_d^l, M_d, M_d^r, F_d^m), and apply the model in the normal way.
- All SDOF model parameters which depend on the static strengths (M_p^l, M_p, M_p^r, F_p^m) should be re-evaluated for the new dynamic values, except for the plastic interaction radii (r_p^l, r_p, r_p^r) which should be kept unchanged.

6 DUCTILITY MEASURES

Plastic strains represent the most commonly applied measure of ductility for steel members. In the presence of material rate sensitivity, the plastic hinges become finite in length, where the plastic hinge region is defined as that over which the static plastic bending moment capacity is exceeded under dynamic loading. Accordingly, plastic strains can be determined from knowledge of the plastic rotation and extension of a plastic hinge, accounting for concentration effects due to the variation of bending moments over the plastic hinge. An improved method is proposed here, which overrides the previous approximate approach that did not account for rate sensitivity, where the plastic strains developed in the member can be evaluated at various stages of the response.

The following points should be considered when applying the above table:

- Plastic strains are assumed to be induced in the member at its ends only if the plastic moment capacities of the supports are equal (not less) than the static member moment capacity M_p , such conditions being considered *statically*. Therefore, the table is naturally intended for plastic-strain evaluation in the member plastic hinges, and not for those which lie in the supports.
- Axial extension at a plastic hinge is considered subject to a further *static* condition that the axial resistance of the hinge exceeds the overall axial resistance (F_p^m). For a plastic hinge at the member ends, the violation of this condition implies that axial plasticity is mainly concentrated in the support rather than in the member. For an internal plastic hinge, this condition is typically satisfied due to lower axial strength of the supports. However, in rare cases it may be violated, and hence axial plasticity could spread over the full length of the member, though the flexibility of the supports would normally delay the onset of full axial plasticity. Due to such considerations, and with the interest of avoiding excessive model complexity, the case of full axial plasticity spread over the member is excluded in the evaluation of plastic strains.
- The range of midspan displacements v^m considered is that following the initiation of full bending plasticity (i.e. following the end of the second elasto plastic stage: $v^m \geq v_{\max}^{m,ep(2)}$).
- The expressions for the plastic strains at a hinge are determined by the plastic extension, plastic rotation, hinge length, distance y to extreme fibre, and a strain concentration factor which depends on material rate parameter n .
- The plastic hinge lengths are determined by the member length and the normalised dynamic bending strengths.
 - The hinge lengths are taken to be those associated with the bending collapse mechanism, covering the regions over which the dynamic bending moments exceed the static yield limit. The use of the yield instead of the plastic moment in the evaluation of plastic-hinge lengths is an empirical device which allows the current ductility model to be applied for low as well as high displacement rates, thus subsuming the previous rate-insensitive ductility model.

- The variation in the hinge lengths due to catenary action is ignored. Allowing for such a variation would increase the complexity of the procedure without a commensurate improvement in the estimation of plastic strains.
- The normalised dynamic bending strength are defined as the ratio of the dynamic capacity to the member static bending moment capacity:

$$(25): \quad m_d^l = \frac{M_d^l}{M_y}, \quad m_d = \frac{M_d}{M_y}, \quad m_d^r = \frac{M_d^r}{M_y}, \quad m_d^t = \sqrt{(m_d + m_d^l)(m_d + m_d^r)}$$

where M_y is the static yield moment capacity.

- The plastic hinge rotations are determined accounting for the overall and elastic member deformations. In evaluating these rotations, the reduced plastic bending strengths should be based on the dynamic rather than the static values:

$$(27): \quad M_{ps}^l = M_d^l - M_0^l, \quad M_{ps} = M_d - M_0, \quad M_{ps}^r = M_d^r - M_0^r$$

- The plastic hinge extensions are directly related to the full member extension prior to the catenary stages, where the axial force is zero, and are related to the increments of plastic hinge rotations in the catenary stages.

The proposed method for plastic strain evaluation provides a more realistic assessment than the previous method which ignored rate sensitivity [1]. As mentioned before, the empirical use of M_y instead of M_p in evaluating the plastic-hinge lengths enables the current model to be used for both the rate-sensitive and rate-insensitive responses, though in the latter case the current model predicts higher strain-concentrations than the previous rate-insensitive model, which adopted constant strain-concentration factors of 1 and 2 for the axial and bending plastic strains, respectively.

7 EXAMPLES AND VERIFICATION

The enhancement of the previous SDOF model [1] to account for material rate sensitivity is verified here through comparisons with the nonlinear finite element analysis program ADAPTIC [3]. With the details of determining the SDOF model characteristics in terms of the static bending and axial strengths discussed in previous reports [1], focus is given here to the determination of the dynamic bending and axial strengths, which then simply replace the corresponding static strengths in the original SDOF models. Several dynamic analysis examples are provided for a beam under different boundary conditions and subject to UDL blast loading.

7.1 CROSS-SECTION RESPONSE

In the following examples, a Grade 50 UB 356×171×57 is used for which the following properties apply:

$\begin{aligned} \text{Flanges} &: 172.1 \times 13 \text{ mm}^2, & \text{Web} &: 332.6 \times 8 \text{ mm}^2 \\ EI &= 3.3223 \times 10^7 \text{ N.m}^2, & EA &= 1.4984 \times 10^9 \text{ N} \\ M_p &= 3.5303 \times 10^5 \text{ N.m}, & F_p &= 2.5331 \times 10^6 \text{ N} \\ D &= 40 \text{ sec}^{-1}, & n &= 5 \end{aligned}$

Considering bending about the major axis, and taking d_w as the centre-to-centre distance between the flanges ($d_w = 0.3456 \text{ m}$), d_e and D_κ are determined from (19) and (16) as:

$d_e = 0.1555 \text{ m}, \quad D_\kappa = 257.2 \text{ m}^{-1} \text{ sec}^{-1}$
--

The above values of d_e and D_κ are used for the following examples.

7.2 UDL BLAST

Two examples are provided here to verify the rate-sensitive dynamic response for UDL blast loading, where comparisons are made against ADAPTIC [3]. The UB of Section 10.1 is used, and the member length L is taken as 5m. The beam is assumed to have a uniformly distributed mass with a total value mL of 10^4 kg , and is subjected to a triangular loading pulse with a rise time and duration of 10 msec and 100 msec, respectively, where the peak value of the total load P_{\max} is varied for the particular problem. Two sets of support conditions, used previously for verifying the original rate-insensitive model [1], are considered hereafter. It is noted that in all cases, no adjustment is made to the reference velocity at the transition between different resistance stages (Section 9).

Support conditions: set (3)

This case ignores the catenary stage, where the support boundary conditions are as follows:

$\begin{aligned} K_m^1 &= 7.9734 \times 10^7 \text{ N.m}, & K_m^r &= 1.9934 \times 10^7 \text{ N.m} \\ M_p^1 &= 1.7652 \times 10^5 \text{ N.m}, & M_p^r &= 3.5303 \times 10^5 \text{ N.m} \end{aligned}$
--

leading to the intermediate parameters:

$$k_m^l = 12, \quad k_m^r = 3$$

Considering first the rate-insensitive response, generic bending case **B2** is applicable, where the resulting response characteristics are [1]:

	Elastic	Elasto-plastic(1)	Elasto-plastic(2)	Plastic
k (N/m)	5.1030×10^7	2.9160×10^7	4.4374×10^6	0
R_{\max} (N)	4.2364×10^5	8.9435×10^5	9.8849×10^5	9.8849×10^5
v_{\max}^m (m)	8.3017×10^{-3}	2.4444×10^{-2}	4.5660×10^{-2}	-
K_{LM}	0.7760	0.7850	0.6623	0.6667
V^l (N)	0.4139R + ... 0.1277P	0.350R + ... 0.0875P + ... 4.4129×10^4	0.1264R + ... 0.1236P + ... 2.1182×10^5	0.125P + ... 3.3528×10^5
V^r (N)	0.3592R + ... 0.0991P	0.4507R + ... 0.1118P - ... 4.4129×10^4	0.6089R + ... 0.1411P - ... 2.1182×10^5	0.125P + ... 4.0599×10^5

Under a peak total load P_{\max} of 2×10^6 N, the rate-insensitive response is depicted in Figure 8, where very good comparison is observed against the results of ADAPTIC. The average displacement rate up to the peak deflection is around 4m/sec, but allowing for a reduction in the response due to high strain-rate, a reduced value ($\dot{v}^m = 2$ m/sec) is assumed next for the rate-sensitive response.

With ($M_p^l < M_p$), the left plastic hinge is in the support, and hence the corresponding rate-sensitivity parameters are assumed to be given as:

$$D_\theta^l = 53.58 \text{sec}^{-1}, \quad n_m^l = 6$$

Considering Table 3 for the remaining plastic hinges, the following parameters are obtained:

$$\begin{aligned} \alpha &= 0.3694 \\ m_p^l &= 0.5, & m_p^r &= 1.0 \\ D_\theta &= 360.0 \text{sec}^{-1}, & D_\theta^r &= 28.91 \text{sec}^{-1} \\ n_m &= 5.5, & n_m^r &= 6 \end{aligned}$$

which in combination with Tables 4 and 1 leads to the dynamic bending strengths:

$$\begin{aligned} \dot{\theta}_p^l &= 0.8 \text{sec}^{-1}, & \dot{\theta}_p &= 1.6 \text{sec}^{-1}, & \dot{\theta}_p^r &= 0.8 \text{sec}^{-1} \\ M_d^l &= 2.641 \times 10^5 \text{ N.m}, & M_d &= 4.849 \times 10^5 \text{ N.m}, & M_d^r &= 5.472 \times 10^5 \text{ N.m} \end{aligned}$$

Re-applying the SDOF model with (M_p^l, M_p, M_p^r) replaced by (M_d^l, M_d, M_d^r) , generic bending case **B2** is still applicable, and the following rate-sensitive response characteristics are obtained:

	Elastic	Elasto-plastic(1)	Elasto-plastic(2)	Plastic
k (N/m)	5.1030×10^7	2.9160×10^7	4.4374×10^6	0
R_{\max} (N)	6.3386×10^5	1.2457×10^6	1.4249×10^6	1.4249×10^6
v_{\max}^m (m)	1.2421×10^{-2}	3.3405×10^{-2}	7.3776×10^{-2}	-
K_{LM}	0.7760	0.7850	0.6623	0.6667
V^l (N)	$0.4139R + \dots$ $0.1277P$	$0.350R + \dots$ $0.0875P + \dots$ 6.6027×10^4	$0.1264R + \dots$ $0.1236P + \dots$ 2.9960×10^5	$0.125P + \dots$ 4.7771×10^5
V^r (N)	$0.3592R + \dots$ $0.0991P$	$0.4507R + \dots$ $0.1118P - \dots$ 6.6027×10^4	$0.6089R + \dots$ $0.1411P - \dots$ 2.9960×10^5	$0.125P + \dots$ 5.9095×10^5

Using the modified SDOF model characteristics, the predicted rate-sensitive response is shown in Figure 8, where excellent comparison is obtained against the results of ADAPTIC, with rate sensitivity shown to lead to over 50% reduction in the maximum achieved displacement. Favourable comparison is also demonstrated for the reactions in Figure 9, with the small discrepancies attributed to high frequency components that are not typically reflected by a SDOF model.

The plastic strains are evaluated for the plastic hinges within the member, at midspan and at the right end, according to Table 5, where the following intermediate parameters are obtained:

$M_y = 3.1323 \times 10^5$ N.m,	$y = 0.1793$ m
$m_d^l = 0.8432$,	$m_d = 1.5481$
$m_d^r = 1.7469$,	$m_d^t = 2.8070$

In the range of displacements relevant to this example ($v^m \in [v_{\max}^{m,ep(2)} \rightarrow r_p^t]$), the plastic strains are obtained as:

	Internal plastic hinge	Right plastic hinge
Plastic-hinge rotation (rad) θ_p, θ_p^r	$-0.02532 + 0.8 v^m$	$-0.02951 + 0.4 v^m$
Plastic-hinge extension (m) Δ_p, Δ_p^r	$0.22857 (v^m)^2$	$0.11429 (v^m)^2$
Plastic-hinge length (m) h_p, h_p^r	2.2023	0.3257
Plastic strain $\varepsilon_p, \varepsilon_p^r$	$-0.00558 + 0.17631 v^m + \dots$ $0.28096 (v^m)^2$	$-0.09748 + 1.3214 v^m + \dots$ $2.1056 (v^m)^2$

The following table compares the maximum plastic strains from the proposed model with those predicted by ADAPTIC at a specific displacement ($v^m = 0.1768\text{ m}$):

	Internal plastic hinge	Right plastic hinge
Plastic strain (SDOF model) $\varepsilon_p, \varepsilon_p^r$	0.03436	0.20187
Plastic strain (ADAPTIC) $\varepsilon_p, \varepsilon_p^r$	0.03146	0.14466

Reasonable comparison is observed in the above table between the plastic-strain predictions of the proposed SDOF model and those of ADAPTIC. The discrepancy in the large plastic strain at the right support is mainly attributed to the use of a 3-parameter rate-sensitive material model [4] in ADAPTIC, which provides a very good overall fit of the Cowper-Symonds model, but which typically leads to lower strain concentrations. It should also be noted that much lower plastic strains would be achieved if a small amount of material strain hardening is included, though this has been outside the scope of the current SDOF model development. Considering a bilinear stress-strain model for steel with a post-yield strain-hardening slope of 2% of the elastic modulus (E), much reduced plastic strains are achieved with ADAPTIC at a maximum displacement ($v^m = 0.1483\text{ m}$), which compare as follows to the predictions of the current SDOF model:

	Internal plastic hinge	Right plastic hinge
Plastic strain (SDOF model) $\varepsilon_p, \varepsilon_p^r$	0.02675	0.14478
Plastic strain (ADAPTIC) $\varepsilon_p, \varepsilon_p^r$	0.02152	0.04629

Clearly, therefore, a more realistic assessment of plastic strains with the SDOF model requires its further extension to account for material strain hardening.

Support conditions: set (4)

This case accounts for the catenary response, where the following rotational and axial support stiffnesses are assumed:

$K_m^l = K_m^r = 0\text{ N.m}$,	$M_p^l = M_p^r = 0\text{ N.m}$
$K_f^l = 1.4984 \times 10^8\text{ N/m}$,	$K_f^r = 1.4984 \times 10^8\text{ N/m}$
$F_p^l = 1.2666 \times 10^6\text{ N}$,	$F_p^r = 2.5331 \times 10^6\text{ N}$

leading to the following intermediate parameters:

$$\begin{aligned} k_m^l = k_m^r = 0, \quad r_p^l = r_p^r = 0 \text{ m} \\ r_p = r_p^l = 0.13937 \text{ m}, \quad K_f^e = 5.9937 \times 10^7 \text{ N/m} \\ F_p^m = 1.2666 \times 10^6 \text{ N}, \quad d_p^m = 0.45969 \text{ m} \end{aligned}$$

Considering first the rate-insensitive response, generic bending case **B3** is applicable, where the last two elasto-plastic bending stages are ignored since the corresponding support rotational stiffnesses are zero. The resulting response characteristics, accounting for the bending and catenary stages with the nonlinear catenary model, are obtained as:

	Elastic	Plastic	Catenary (1)	Catenary (2)
k (N/m)	2.0412×10^7	0	$3.8360 \times 10^7 (v^m - 0.13937)^2$	2.0265×10^6
k_s (N/m)				
R_{\max} (N)	5.6485×10^5	5.6485×10^5	1.0306×10^6	-
v_{\max}^m (m)	2.7673×10^{-2}	0.13937	0.36921	-
K_{LM}	0.7873	0.6667	0.6667	0.6667
V^l & V_r (N)	$0.4065R + \dots$ $0.0935P$	$0.1250P + \dots$ 2.1182×10^5	$0.3750R + \dots$ $0.1250P$	$0.3750R + \dots$ $0.1250P$

The beam is analysed with the SDOF model, for a peak load P_{\max} of 2×10^6 N, where the predicted rate-insensitive response is compared favourably to the ADAPTIC results in Figure 10. The average displacement rate up to the peak deflection is around 6 m/sec, but allowing for a reduction in the response due to high strain-rate, a reduced value ($\dot{v}^m = 4$ m/sec) is assumed next for the rate-sensitive response.

With ($F_p^l < F_p^r = F_p$), full axial plasticity is concentrated in the left support, for which the rate-sensitivity parameters are assumed to be given, leading to the following axial parameters according to Table 2:

$$D_{\Delta}^m = D_{\Delta}^l = 50 \text{ m/sec}, \quad n_f^m = n_f^l = 5$$

Noting that the bending-rate parameters for the support plastic hinges are not required, since their static bending strengths are zero, the parameters associated with the internal plastic hinge are obtained from Table 3 as:

$$\begin{aligned} \alpha = 0.3694 \\ m_p^l = 0, \quad m_p^r = 0 \\ D_{\theta} = 475.0 \text{ sec}^{-1}, \quad n_m = 5.5 \end{aligned}$$

which in combination with Tables 4, 1 and 2 leads to the following dynamic strengths:

$$\begin{aligned} \dot{\theta}_p &= 3.2 \text{ sec}^{-1}, & \dot{\Delta}_p^t &= 1.1815 \text{ m/sec}, & \dot{\Delta}_p^m &= 0.7355 \text{ m/sec} \\ M_d^l &= M_d^r = 0 \text{ N.m}, & M_d &= 4.9526 \times 10^5 \text{ N.m}, & F_d^m &= 1.8112 \times 10^6 \text{ N} \end{aligned}$$

Re-applying the SDOF model with $(M_p^l, M_p, M_p^r, F_p^m)$ replaced by $(M_d^l, M_d, M_d^r, F_d^m)$, generic bending case **B3** is still applicable, and d_p^m is recalculated as:

$$d_p^m = 0.54971 \text{ m}$$

The resulting SDOF response characteristics become:

	Elastic	Plastic	Catenary (1)	Catenary (2)
k (N/m)	2.0412×10^7	0	$3.8360 \times 10^7 (v^m - 0.13937)^2$	2.8979×10^6
k_s (N/m)				
R_{\max} (N)	7.9242×10^5	7.9242×10^5	1.5889×10^6	-
v_{\max}^m (m)	3.8822×10^{-2}	0.13937	0.41423	-
K_{LM}	0.7873	0.6667	0.6667	0.6667
V^l & V_r (N)	$0.4065 R + \dots$ $0.0935 P$	$0.1250 P + \dots$ 2.9716×10^5	$0.3750 R + \dots$ $0.1250 P$	$0.3750 R + \dots$ $0.1250 P$

Using the modified SDOF model characteristics, the predicted rate-sensitive response is shown in Figure 10, where good comparison is obtained against the results of ADAPTIC, again demonstrating the significance of the strain-rate effect. Favourable comparison is also shown for the reactions in Figure 11, where the small discrepancies are again attributed to high frequency components that are not typically reflected by a SDOF model.

8 CONCLUSION

This work presents the second-stage extension of a recently developed SDOF model [1] for steel members subject to explosion loading, which was shown to provide significant improvements over other existing models. The proposed model [1] considered i) general support conditions both in terms of flexibility and strength, and ii) catenary action resulting from axial restraint at the supports, under uniformly distributed (UDL), blast loading. However, the model neglected the effect of material rate-sensitivity, which is very important for steel members subject to blast loading. The aim of this second-stage of model extension is to address this shortcoming, and to provide more rational ductility measures than provided with the previous rate-insensitive model.

The report presents an overview of the problem characteristics, and outlines the formulation method employed in developing the advanced SDOF model for dealing with material rate sensitivity. Firstly, the strain-rate effect is dealt with on a cross-sectional level, where relevant parameters are established for a general I-section, subject to bending about the major or minor axis, and for a corrugated wall section. Subsequently, the implications of material rate sensitivity are addressed on a member level, where the dynamic strengths are established for both the bending and catenary stages in terms of the reference displacement rate. As in the previous work [1,2], details of the SDOF model in relation to the dynamic bending and axial strengths are presented in parametric tables specific to each type of blast loading.

The application of the extended SDOF model is illustrated through several examples, where comparisons are made against the predictions of the nonlinear finite element analysis program ADAPTIC [3]. In general, it is shown that the proposed model provides very good accuracy in comparison with ADAPTIC, and demonstrates that the strain-rate effect for steel members subject to blast can reduce the maximum deflection by well over 50%. Importantly, the model enhancement and accuracy are achieved through a reasonably simple formulation, which is very well suited for practical application.

Finally, through the major enhancements incorporated in the proposed SDOF model, a more realistic assessment of steel members subject to explosion loading is now possible using simplified analysis, considering a variety of blast load configurations and combinations with initial static loading, and accounting for the important effect of the strain-rate.

APPENDIX 1 REFERENCES

- [1] B.A. Izzuddin, 2001, 'An Improved SDOF Model for Steel Members Subject to Explosion Loading – Generalised Supports and Catenary Action', Report prepared for the Steel Construction Institute.
- [2] FABIG Guidance Document, 1993, 'Design Guidance for Explosion Loading', Document No. 390, The Steel Construction Institute.
- [3] B.A. Izzuddin, 1991, 'Nonlinear Dynamic Analysis of Framed Structures', PhD Thesis, Department of Civil Engineering, Imperial College, University of London.
- [4] B.A. Izzuddin and Q. Fang, 1997, 'Rate-Sensitive Analysis of Framed Structures - Part I: Model Formulation and Verification', Structural Engineering and Mechanics, Vol. 5, No. 3, pp. 221-237.

APPENDIX 2 NOTATION

A_f^b	Bottom flange area for I-section.
A_f^t	Top flange area for I-section.
A_w	Web area for I-section.
α	Member rate parameter for UDL blast.
b_f^b	Bottom flange width for I-section.
b_f^t	Top flange width for I-section.
d_e	Effective distance from neutral axis for the cross-section rate-sensitive response.
d_p^m	Catenary extension entity.
d_w	Web depth (centre-to-centre of flanges).
D	Material rate parameter.
D_κ	Cross-sectional bending rate parameter.
D_Δ^l	Axial rate parameter for left support plastic hinge.
D_Δ^m	Overall member axial rate parameter.
D_Δ^r	Axial rate parameter for right support plastic hinge.
D_θ	Bending member rate parameter for internal plastic hinge.
D_θ^l	Bending rate parameter for left plastic hinge.
D_θ^r	Bending rate parameter for right plastic hinge.
Δ_p	Plastic extension at internal hinge.
Δ_p^l	Plastic extension at left hinge.
$\dot{\Delta}_p^m$	Local axial extension rate.
Δ_p^r	Plastic extension at right hinge.
Δ_p^t	Total plastic extension over the member and supports.
$\dot{\Delta}_p^t$	Total plastic extension rate over the member and supports.
Δ^t	Total extension over the member and supports.
EA	Elastic axial rigidity of beam.
EI	Elastic bending rigidity of beam.

$\dot{\varepsilon}$:	Strain rate.
$\dot{\varepsilon}_{cp}$:	Centroidal plastic strain rate.
ε_p :	Extreme fibre plastic strain at internal hinge.
$\dot{\varepsilon}_p$:	Plastic strain rate.
ε_p^l :	Extreme fibre plastic strain at left support.
ε_p^r :	Extreme fibre plastic strain at right support.
F :	Axial force.
F_d :	Dynamic plastic axial force capacity of beam.
F_d^m :	Overall dynamic plastic axial capacity.
F_p :	Static plastic axial force capacity of beam.
F_p^l :	Static plastic axial force capacity of left support ($\leq F_p$).
F_p^m :	Overall static plastic axial capacity (minimum of F_p^l , F_p and F_p^r).
F_p^r :	Static plastic axial force capacity of right support ($\leq F_p$).
h_p :	Internal plastic hinge length.
h_p^l :	Plastic hinge length at left support.
h_p^r :	Plastic hinge length at right support.
k :	Stiffness of piecewise linear response segment.
k_m^l :	Normalised elastic rotational stiffness of left support ($K_m^l/(EI/L)$).
k_m^r :	Normalised elastic rotational stiffness of right support ($K_m^r/(EI/L)$).
k_s :	Secant stiffness for nonlinear catenary model.
K_f^e :	Overall elastic axial stiffness (depends on EA/L , K_f^l and K_f^r).
K_f^l :	Elastic axial stiffness of left support.
K_f^r :	Elastic axial stiffness of right support.
K_{LM} :	Load-mass transformation factor associated with uniformly distributed mass.
K_m^l :	Elastic rotational stiffness of left support.
K_m^r :	Elastic rotational stiffness of right support.
$\dot{\kappa}_p$:	Plastic curvature rate.
L :	Length of beam.

m :	Uniformly distributed mass per unit length.
m_d :	Normalised dynamic plastic moment capacity of internal hinge (M_d / M_p).
m_d^l :	Normalised dynamic plastic moment capacity of left support (M_d^l / M_p).
m_d^r :	Normalised dynamic plastic moment capacity of right support (M_d^r / M_p).
m_d^t :	Normalised dynamic plastic moment entity for UDL blast.
m_p^l :	Normalised static plastic moment capacity of left support (M_p^l / M_p).
m_p^r :	Normalised static plastic moment capacity of right support (M_p^r / M_p).
M :	Bending moment.
M_0 :	Internal bending moment due to initial static load.
M_0^l :	Left support bending moment due to initial static loading.
M_0^r :	Right support bending moment due to initial static loading.
M_d :	Dynamic plastic bending moment capacity of beam.
M_p :	Static plastic bending moment capacity of beam.
M_{ps} :	Reduced bending moment capacity of beam ($M_p - M_0$).
M_p^l :	Static plastic bending moment capacity of left support ($\leq M_p$).
M_{ps}^l :	Reduced bending moment capacity of left support ($M_p^l - M_0^l$).
M_p^r :	Static plastic bending moment capacity of right support ($\leq M_p$).
M_{ps}^r :	Reduced bending moment capacity of right support ($M_p^r - M_0^r$).
M_y :	Static yield moment capacity of beam (M_p / s).
n :	Material rate parameter.
n_f^l :	Axial rate parameter for left support plastic hinge.
n_f^m :	Overall member axial rate parameter.
n_f^r :	Axial rate parameter for right support plastic hinge.
n_m :	Member bending rate parameter for internal plastic hinge.
n_m^l :	Bending rate parameter for left plastic hinge.
n_m^r :	Bending rate parameter for right plastic hinge.
P_0 :	Initial static load.
P_{max} :	Peak value of total load.

θ_p	: Plastic rotation at internal hinge.
$\dot{\theta}_p$: Plastic rotation rate at internal hinge.
θ_p^l	: Plastic rotation at left hinge.
$\dot{\theta}_p^l$: Plastic rotation rate at left hinge.
θ_p^r	: Plastic rotation at right hinge.
$\dot{\theta}_p^r$: Plastic rotation rate at right hinge.
r_p	: Plastic interaction radius for beam (M_p / F_p).
r_p^l	: Plastic interaction radius for left support (M_p^l / F_p^l).
r_p^r	: Plastic interaction radius for right support (M_p^r / F_p^r).
r_p^t	: Overall plastic interaction radius.
R	: Static resistance beyond requirement of initial static load.
R_{\max}	: Resistance limit for piecewise response segment.
s	: Section shape factor (S_x / Z_x).
S_x	: Section plastic modulus.
σ_d	: Dynamic yield strength.
σ_y	: Static yield strength.
t	: Time.
v^m	: Reference transverse displacement beyond initial static value.
\dot{v}^m	: Reference displacement rate.
v_0^m	: Reference transverse displacement due to initial static loading.
v_{\max}^m	: Reference displacement limit for piecewise response segment.
$v_{\max}^{m,ep(2)}$: Maximum reference displacement at the end of the final elasto-plastic stage.
V_0^l	: Reaction at left support due to initial static loading.
V_0^r	: Reaction at right support due to initial static loading.
V^l	: Reaction at left support beyond initial static value ($V_s^l + V_d^l$).
V^r	: Reaction at right support beyond initial static value ($V_s^r + V_d^r$).
V_s^l	: Quasi-static reaction at left support beyond initial static value.
V_s^r	: Quasi-static reaction at right support beyond initial static value.

- V_d^l : Dynamic reaction component at left support beyond initial static value.
- V_d^r : Dynamic reaction component at right support beyond initial static value.
- x_{PT} : Location of internal bending hinge, expressed as an x-coordinate.
- y : Distance of material fibre from centroidal reference axis; refers to extreme fibre for plastic-strain evaluation.
- Z_x : Section elastic modulus.

APPENDIX 3 FIGURES

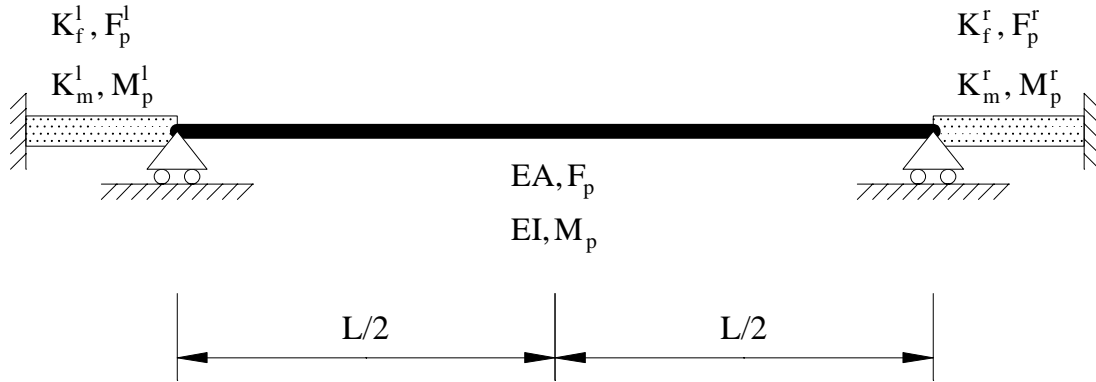


Figure 1 Geometric configuration, boundary conditions and loading configurations

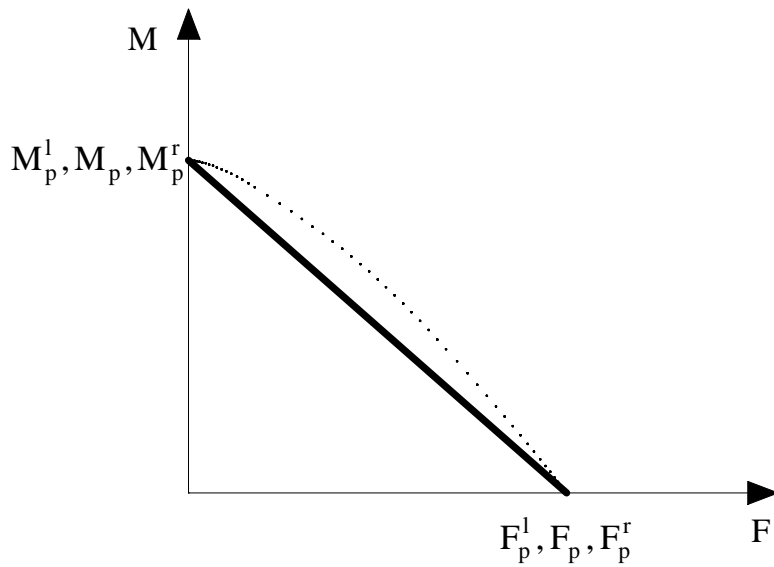


Figure 2 Plastic interaction between axial force and bending moment

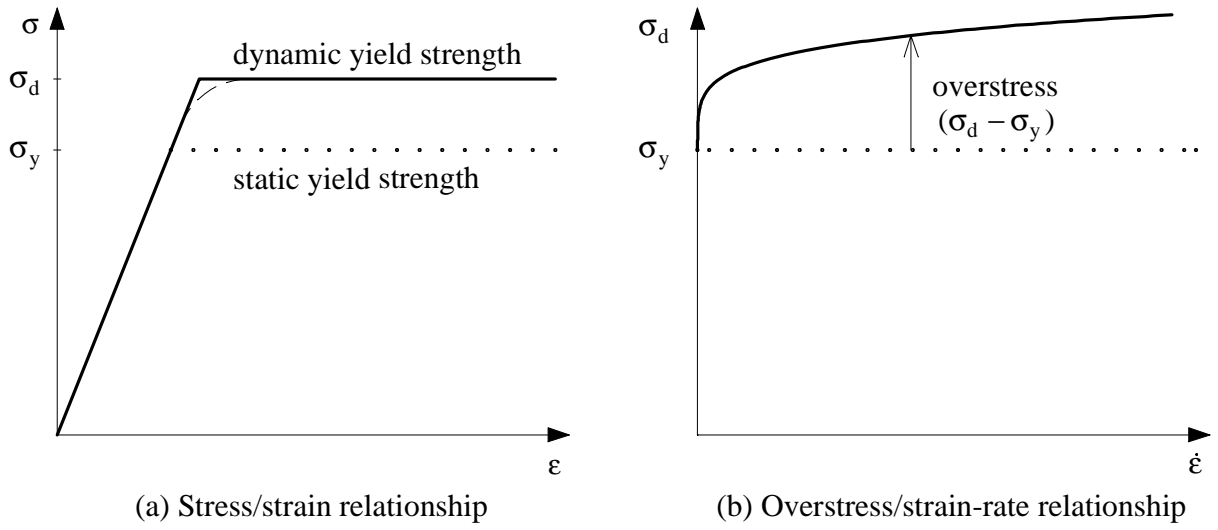


Figure 3 Material response under constant strain rate

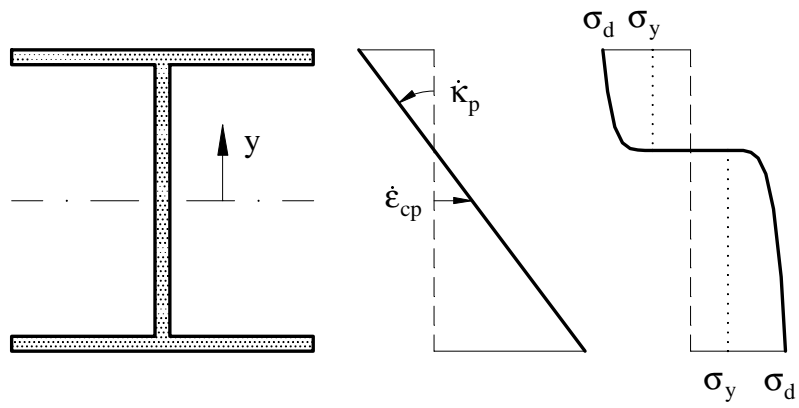


Figure 4 Cross-sectional plastic stress distribution

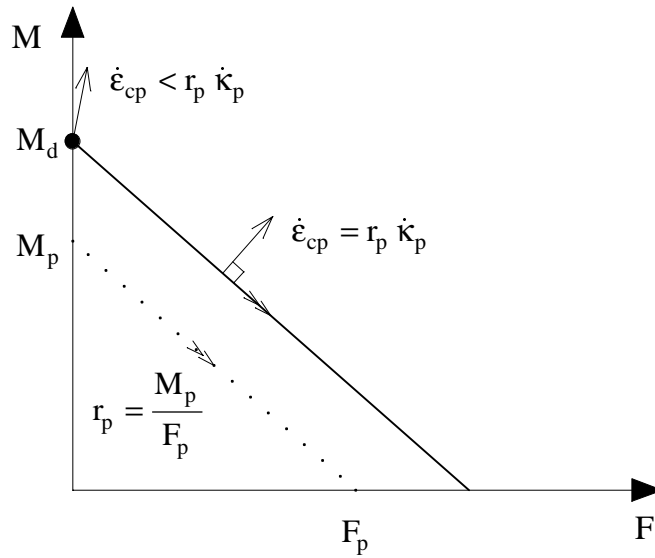


Figure 5 Rate-sensitive interaction between plastic bending moment and axial force

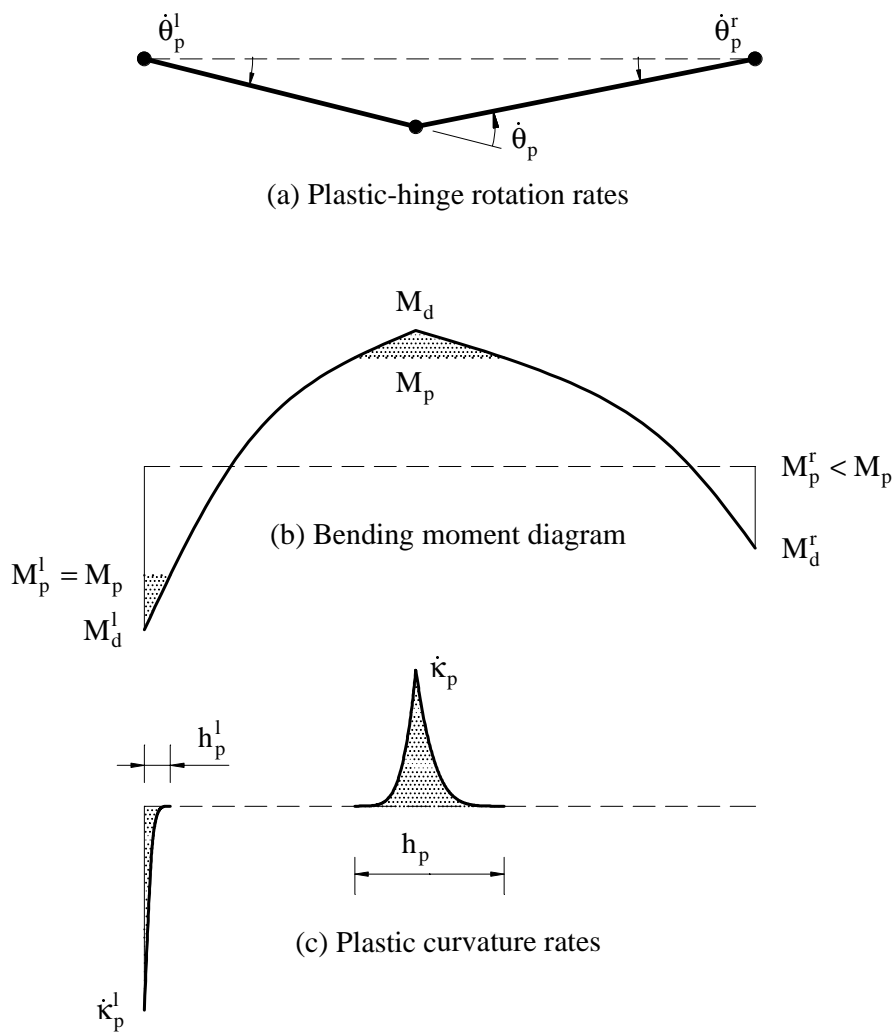
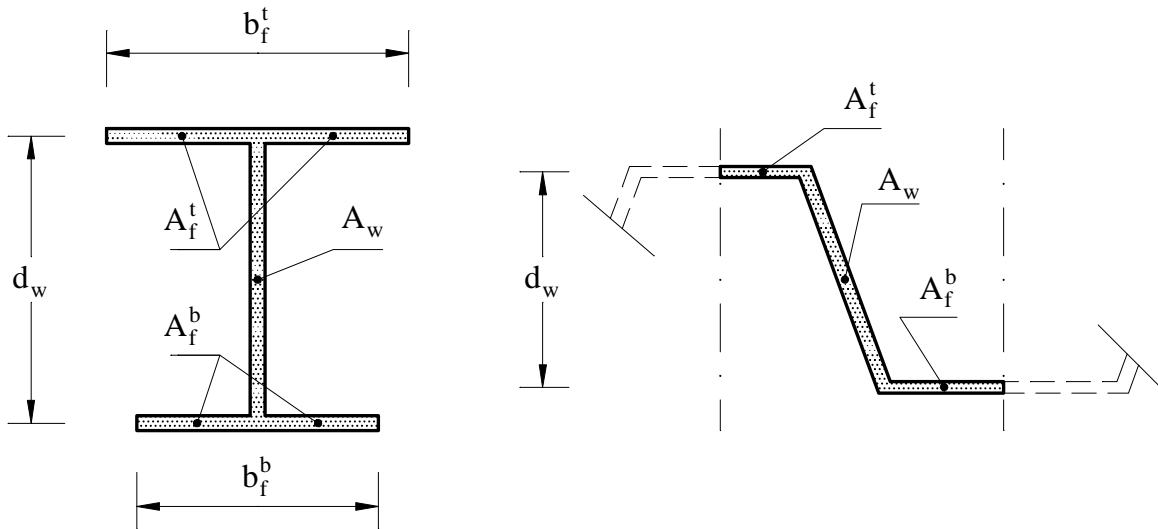


Figure 6 Rotation and curvature rates in plastic bending response



(a) Asymmetric I-section (b) Corrugated wall section

Figure 7 Cross-sectional configurations

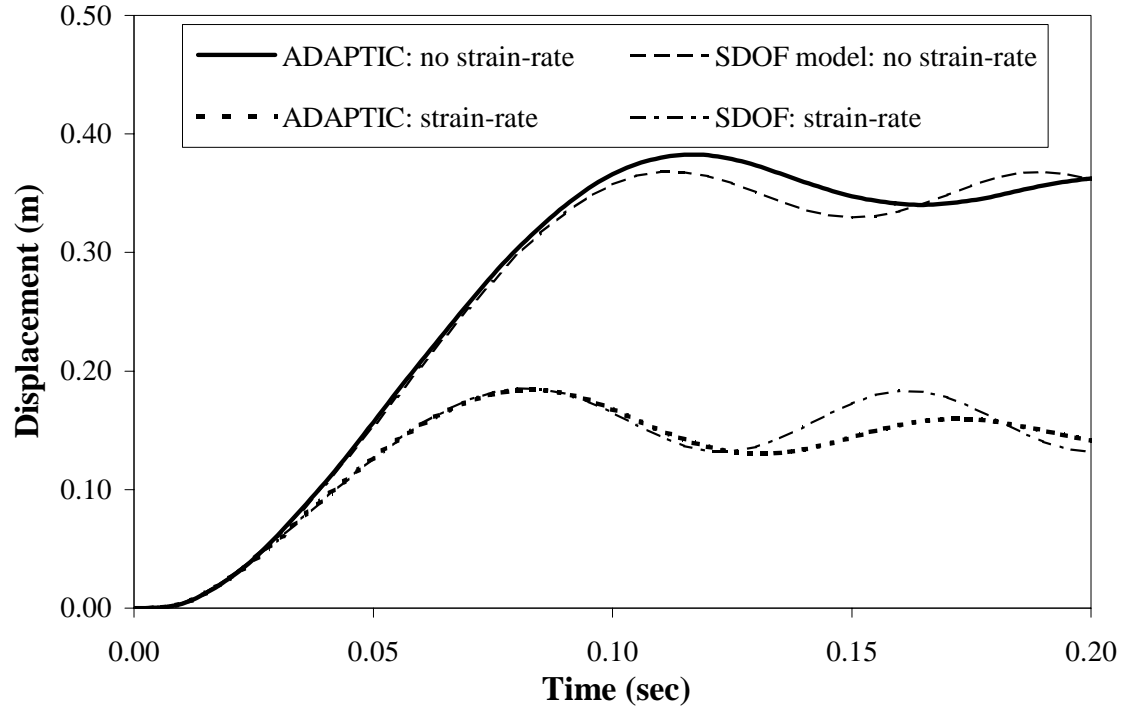


Figure 8 Dynamic response for UDL blast loading: set (3) support conditions

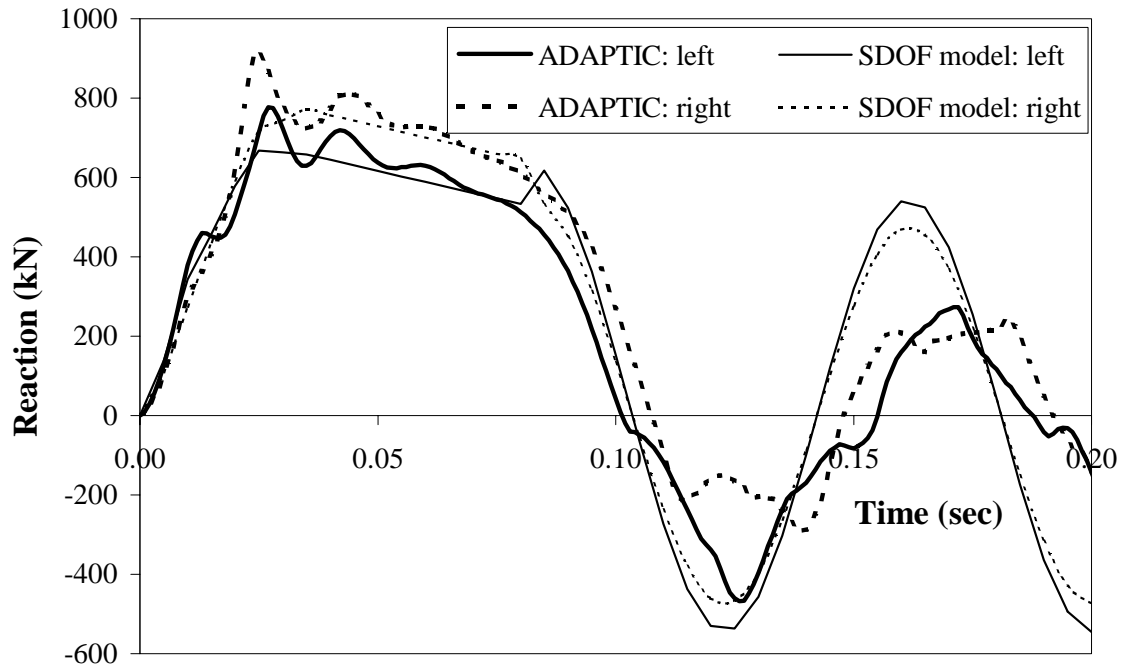


Figure 9 Rate-sensitive reactions for UDL blast loading: set (3) support conditions

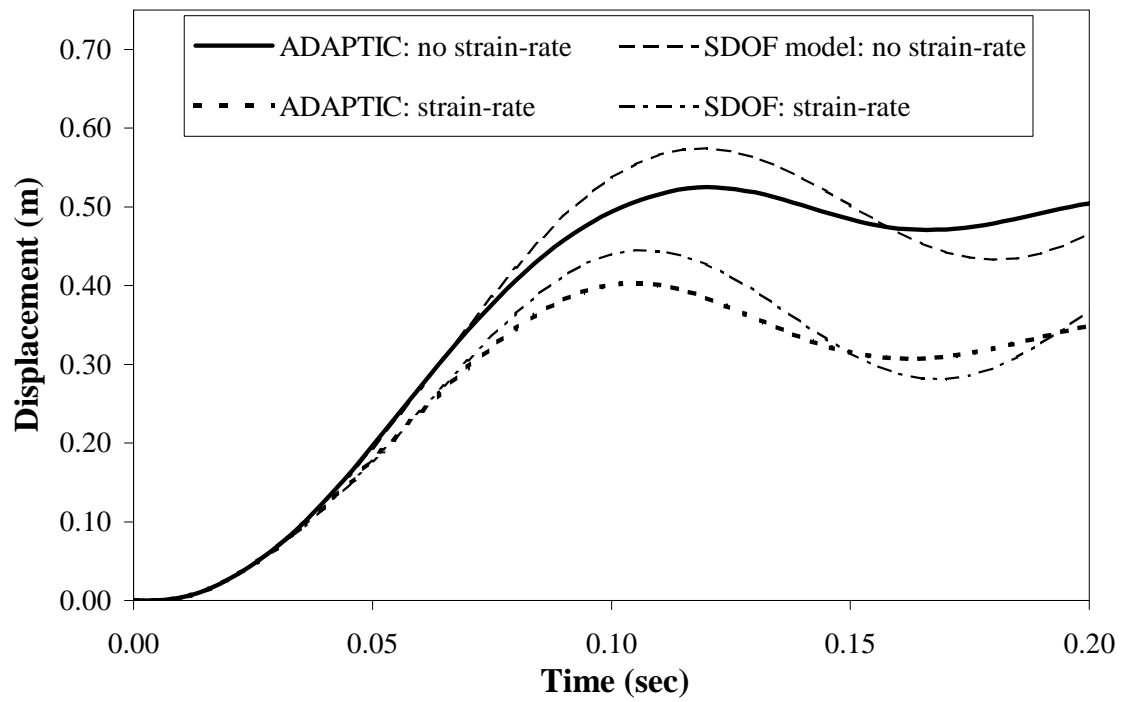


Figure 10 Dynamic response for UDL blast loading: set (4) support conditions

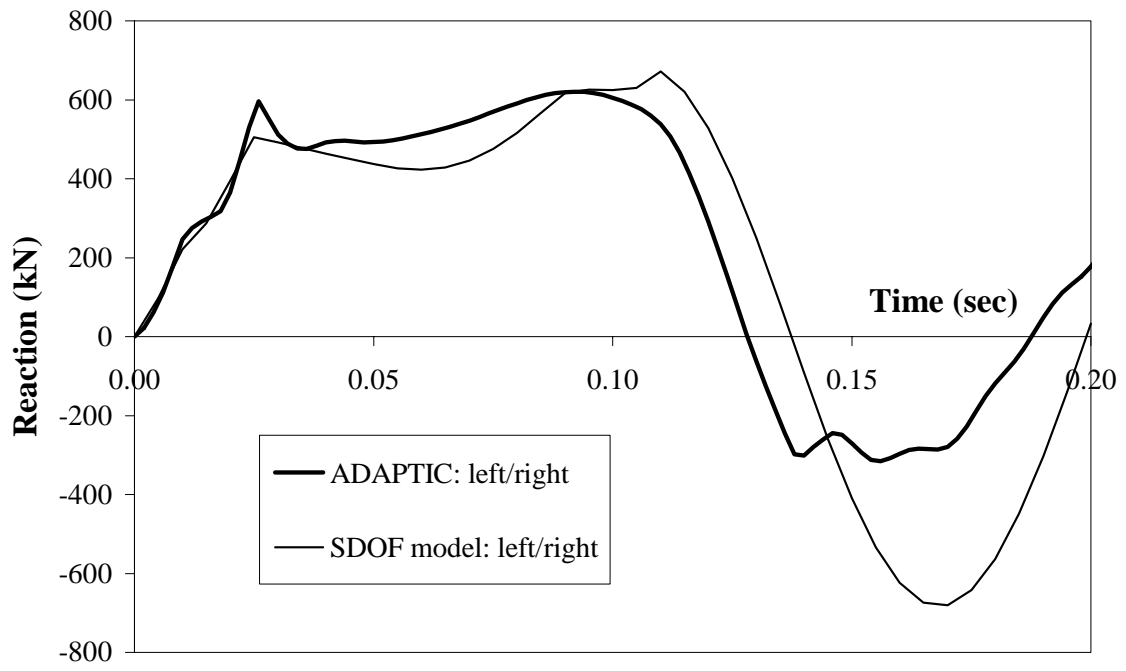


Figure 11 Rate-sensitive reactions for UDL blast loading: set (4) support conditions

APPENDIX 4 TABLES

Table 1 Dynamic bending strengths

Left plastic hinge M_d^l	Internal plastic hinge M_d	Right plastic hinge M_d^r
$M_p^l \left(1 + \left(\frac{\dot{\theta}_p^l}{D_\theta^l} \right)^{1/n_m} \right)$	$M_p \left(1 + \left(\frac{\dot{\theta}_p}{D_\theta} \right)^{1/n_m} \right)$	$M_p^r \left(1 + \left(\frac{\dot{\theta}_p^r}{D_\theta^r} \right)^{1/n_m} \right)$

Table 2 Overall dynamic axial strength

Location of axial plasticity	Left support $F_p^l < F_p^r \leq F_p$	Both supports $F_p^l = F_p^r < F_p$	Right support $F_p^r < F_p^l \leq F_p$	Member $F_p^l = F_p^r = F_p$
Rate parameter D_Δ^m	D_Δ^l	$2D_\Delta^l$	D_Δ^r	DL
Power parameter n_f^m	n_f^l	n_f^l	n_f^r	n
Local axial rate $\dot{\Delta}_p^m$	$\dot{\Delta}_p^l - r_p \dot{\theta}_p^l - r_p^r \dot{\theta}_p^r$	$\dot{\Delta}_p^l - r_p \dot{\theta}_p$	$\dot{\Delta}_p^r - r_p^l \dot{\theta}_p^l - r_p \dot{\theta}_p$	$\dot{\Delta}_p^t$
Axial strength F_d^m	$F_p^m \left(1 + \left(\frac{\dot{\Delta}_p^m}{D_\Delta^m} \right)^{1/n_f^m} \right)$			

Table 3 Bending rate-sensitivity parameters (UDL)

	Left plastic hinge (Condition: $M_p^l = M_p$)	Internal plastic hinge	Right plastic hinge (Condition: $M_p^r = M_p$)
Rate parameter $D_\theta^l, D_\theta, D_\theta^r$	$\frac{D_\kappa L}{(n+1)(1.172 m_p^r + 6.828)}$	$\frac{2 \alpha D_\kappa L}{\sqrt{m_p^l + m_p^r + 2 + 2\sqrt{(m_p^l + 1)(m_p^r + 1)}}$	$\frac{D_\kappa L}{(n+1)(1.172 m_p^l + 6.828)}$
Power parameter n_m^l, n_m, n_m^r	$n+1$	$n + \frac{1}{2}$	$n+1$

Table 4 Plastic deformation rates (UDL)

Left hinge rotation $\dot{\theta}_p^l$	Internal hinge rotation $\dot{\theta}_p$	Right hinge rotation $\dot{\theta}_p^r$	Axial deformation $\dot{\Delta}_p^t$
$\frac{2 \dot{v}^m}{L}$	$\frac{4 \dot{v}^m}{L}$	$\frac{2 \dot{v}^m}{L}$	$\left(r_p^t + \frac{d_p^m}{2} \right) \frac{4 \dot{v}^m}{L}$

Table 5 Approximation of plastic strains at hinge locations (UDL)

	Range v^m	Left plastic hinge	Internal plastic hinge	Right plastic hinge
Plastic strain $\varepsilon_p^l, \varepsilon_p, \varepsilon_p^r$	$[v_{\max}^{m,ep(2)} \rightarrow [$	$(n+1) \left(\frac{\Delta_p^l + y \theta_p^l}{h_p^l} \right)$	$\frac{1}{\alpha} \left(\frac{\Delta_p + y \theta_p}{h_p} \right)$	$(n+1) \left(\frac{\Delta_p^r + y \theta_p^r}{h_p^r} \right)$
Plastic-hinge length h_p^l, h_p, h_p^r	$[v_{\max}^{m,ep(2)} \rightarrow [$	$L \frac{\left((m_d + m_d^l) + m_d^t - \dots \right)}{\sqrt{(m_d + 1 + m_d^t)^2 - (m_d^l - 1)(m_d^t - 1)}} \frac{1}{(m_d + m_d^l) + (m_d + m_d^r) + 2m_d^t}$	$2L \frac{\sqrt{(m_d - 1 + m_d^t)^2 - (m_d^l + 1)(m_d^r + 1)}}{(m_d + m_d^l) + (m_d + m_d^r) + 2m_d^t}$	$L \frac{\left((m_d + m_d^r) + m_d^t - \dots \right)}{\sqrt{(m_d + 1 + m_d^t)^2 - (m_d^l - 1)(m_d^r - 1)}} \frac{1}{(m_d + m_d^l) + (m_d + m_d^r) + 2m_d^t}$
Plastic-hinge rotation $\theta_p^l, \theta_p, \theta_p^r$	$[v_{\max}^{m,ep(2)} \rightarrow [$	$\frac{L}{48EI} \left\{ 6M_{ps} - \frac{7k_m^l + 48}{k_m^l} M_{ps}^l + M_{ps}^r \right\} + \frac{2v^m}{L}$	$\frac{L}{24EI} \left\{ -10M_{ps} + M_{ps}^l + M_{ps}^r \right\} + \frac{4v^m}{L}$	$\frac{L}{48EI} \left\{ 6M_{ps} + M_{ps}^l - \frac{7k_m^r + 48}{k_m^r} M_{ps}^r \right\} + \frac{2v^m}{L}$
Static condition	$[v_{\max}^{m,ep(2)} \rightarrow [$	$M_p^l = M_p$	-	$M_p^r = M_p$
Plastic-hinge extension $\Delta_p^l, \Delta_p, \Delta_p^r$	$[v_{\max}^{m,ep(2)} \rightarrow r_p^t - v_0^m]$	$\frac{r_p (v^m + v_0^m)^2}{r_p^t L}$	$\frac{2r_p (v^m + v_0^m)^2}{r_p^t L}$	$\frac{r_p (v^m + v_0^m)^2}{r_p^t L}$
	$[r_p^t - v_0^m \rightarrow [$	$\frac{r_p (2v^m + 2v_0^m - r_p^t)}{L}$	$\frac{2r_p (2v^m + 2v_0^m - r_p^t)}{L}$	$\frac{r_p (2v^m + 2v_0^m - r_p^t)}{L}$
Static condition	$[v_{\max}^{m,ep(2)} \rightarrow [$	$M_p^l = M_p \ \& \ F_p^l > F_p^m$	$F_p > F_p^m$	$M_p^r = M_p \ \& \ F_p^r > F_p^m$

**MAIL ORDER**

HSE priced and free
publications are
available from:

HSE Books
PO Box 1999
Sudbury
Suffolk CO10 2WA
Tel: 01787 881165
Fax: 01787 313995
Website: www.hsebooks.co.uk

RETAIL

HSE priced publications
are available from booksellers

HEALTH AND SAFETY INFORMATION

HSE Infoline
Tel: 0845 345 0055
Fax: 0845 408 9566
Textphone: 0845 408 9577
e-mail: hse.infoline@natbrit.com
or write to:
HSE Information Services
Caerphilly Business Park
Caerphilly CF83 3GG

HSE website: www.hse.gov.uk

RR 435